

A microfluidic device with integrated fluorimetric detection for flow injection analysis

Alexandre Fonseca · Ivo M. Raimundo Jr. ·
Jarbas J. R. Rohwedder · Renato S. Lima ·
Mário C. Ugulino Araújo

Received: 24 August 2009 / Revised: 15 October 2009 / Accepted: 18 October 2009 / Published online: 8 November 2009
© Springer-Verlag 2009

Abstract This work describes the development of flow analysis microsystems with integrated fluorimetric detection cells. Channels (width of 300–540 μm and depth of 200–590 μm) were manufactured by deep-UV lithography in urethane-acrylate (UA) resin. Plastic optical fibers (diameter of 250 μm) were coupled to a 2.0-mm-long detection channel in order to guide the excitation radiation from an LED (470 nm) and collect the emitted radiation at a right angle towards a photomultiplier. A single-line miniaturized system, with a total internal volume of 10.4 μL , was evaluated by means of standard fluorescein solutions (0.53–2.66 $\mu\text{mol L}^{-1}$, pH 8.5). The analytical signals presented a linear relationship in the concentration range studied, with a relative standard deviation of 1.9% ($n=5$), providing a detection limit of 0.37 $\mu\text{mol L}^{-1}$ and an analytical frequency of 60 samples/h, using a flow rate of 60 $\mu\text{L min}^{-1}$. Optical microscopy images and videos acquired in real time for the hydrodynamic injection of 130 and 320 nL of sample solutions indicated the good performance of the proposed sampling strategy. Another microsystem with a total internal volume of 38 μL was developed, incorporating a confluence point for two solutions. This device was applied to the determination of

the total concentration of Ca^{2+} and Mg^{2+} in commercial mineral waters using the calcein method. Microscopy images and videos demonstrated the mixing efficiency of the solutions in the microchannels. A linear relationship was observed for the analytical signal in the Ca^{2+} concentration range from 25 to 125 $\mu\text{mol L}^{-1}$, with relative standard deviations of 3.5%. The analysis of mineral waters with the proposed system provided results that did not differ significantly from those obtained by the EDTA titration method at a confidence level of 95%. These results demonstrate the viability of developing micro flow injection systems with an integrated fluorimetric detection cell.

Keywords μ -TAS · Microfluidics · Flow analysis · UV lithography · Fluorimetry

Introduction

Flow analysis (FA) is the simplest and most robust alternative for automation of wet analytical methods and can be used with practically all the instrumental techniques of detection. Over the last 35 years, it has been verified that the use of this strategy provides a simpler and less expensive way to determine organic and inorganic species, when compared to batch methods [1–3]. Although conventional flow analysis systems present good performance in terms of reagent consumption and residue generation, their miniaturization has been widely studied in recent years as a means of improving such characteristics.

The first attempt to construct a miniaturized FA system was proposed by Ruzicka and Hansen in 1984 [4]; by integrating semicircular channels (0.8 mm^2 cross-section), a sampling system and a detector in a single block of PVC, using the hot embossing technique [5]. Despite the good

Electronic supplementary material The online version of this article (doi:10.1007/s00216-009-3252-4) contains supplementary material, which is available to authorized users.

A. Fonseca · I. M. Raimundo Jr. (✉) · J. J. R. Rohwedder
Instituto de Química, Universidade Estadual de Campinas,
UNICAMP,
Cx Postal 6154, 13084-971 Campinas, São Paulo, Brazil
e-mail: ivo@iqm.unicamp.br

R. S. Lima · M. C. U. Araújo
Departamento de Química, UFPB,
João Pessoa CEP 58059-900, Brazil

analytical results obtained with that system, the large dimensions of its channels limited the improvements over conventional FA systems.

Nowadays, new materials and techniques have been applied to construct such devices with channel dimensions ranging from 20 to 700 μm , providing a significant reduction in the consumption of sample and reagent solutions. Leelasattarakul et al. [6] constructed a glass/poly (dimethylsiloxane) hybrid microsystem with an integrated spectrophotometric detection cell, with channels 50 μm deep and 200 μm wide, by using the wet etching technique [7]. Compared to the usual FA system, the proposed device, applied to the determination of Cu(II) in wastewaters, provides a 200-fold reduction in the consumption of reagents, by using a flow rate of only 10 $\mu\text{L min}^{-1}$ for the carrier stream. Baeza et al. [8] have demonstrated the use of multicommutation to improve the mixing of solutions in a micro flow analyzer made of silicon and glass, by using reactive ion etching and anodic bonding techniques [7]. The microsystem, with channels 200 μm wide and 700 μm deep and an integrated detection cell, was applied for the spectrophotometric determination of nitrite in water. The best results were obtained using a total flow rate of 250 $\mu\text{L min}^{-1}$, which corresponds to 25% of the flow rate usually employed in FA systems. Kruanetr et al. [9] have proposed the use of a microflow analyzer for determination of Fe(III) in waters. The device was constructed by laser ablation of poly(methylmethacrylate), which was joined to a molded PDMS, in order to seal and to provide solution access. Because of the small size of the channels (200 μm wide \times 50 μm deep), the maximum flow rate allowed was 30 $\mu\text{L min}^{-1}$, producing a residue of 2.0 mL/h of work.

One of the most important challenges in developing microfluidic devices is the integration of optical detectors, that allow an adequate management of the electromagnetic radiation and also offers reduction in size, turning the entire system more compact [10, 11]. Due to its high sensitivity and selectivity, spectrofluorimetric detection is among the more popular strategies employed with analytical microchips [12, 13]. However, the literature [10, 11] indicates that its adaptation to the microfluidic world is still complicated mainly due to difficulties in interfacing the optical parts to the microfluidic system. In laser-induced fluorescence (LIF) or lamp-based fluorescence [11] that are frequently employed, lens and optical filters are aligned and used to focus the excitation light on the detection microchannel and to collect the emitted radiation of the fluorophore, so that the great number of mobile parts hinders the use of the microdevices. Despite these drawbacks, some microfluidic systems with fluorimetric detection have been proposed. A monolithic FIA microsystem, which incorporates peristaltic pumps, injection valve and reaction coil, made in PDMS, has been described by Leach et al. [14].

The detection was accomplished by means of an inverted microscope, allowing a detection limit of 4.0×10^{-19} mol for fluorescein, by injecting a sample volume of 1.25 nL. Du et al. [15] have proposed a sequential injection analyzer in a short capillary, furnished with a laser-induced fluorescence detector. The performance of the analyzer was evaluated with fluorescein solutions, showing a linear response from 50 to 250 nmol L^{-1} and a relative standard deviation of 0.8% ($1.0 \mu\text{mol L}^{-1}$, $n=7$). Destandau et al. [16] have developed a Y-shaped microfluidic system in PDMS, with a detection system constituted of a LED as light source and a photomultiplier tube as detector. The system was applied to determination of potassium ions, presenting a detection limit of 0.5 mmol L^{-1} .

Recently, the integration of optical fibers to microfluidic devices has been proposed to simplify the detection system by minimizing the number of optical components. In this approach, channels are manufactured into the microchip and used to introduce optical fibers that allow optical detection [11]. Using this approach, we have recently proposed [17] the construction of a microanalyzer based on urethane-acrylate (UA) resin, with an integrated photometric flow cell implemented by connecting plastic optical fibers (diameter of 250 μm) at the ends of a 5.0-mm-long channel, which acted as optical path. The alignment of the fibers was easily attained by using pre-fabricated channels to guide and hold the fibers in the microsystem, dispensing the use of lens and alignment apparatus, usually necessary for this task.

In the present work, urethane-acrylate flow injection microsystems with integrated fluorimetric detection cells, implemented with the use of optical fibers, are described. The performances of the proposed microsystems were evaluated with fluorescein reference solutions and the optimized system was applied to the determination of total Ca^{2+} and Mg^{2+} in mineral waters. The efficiency of the hydrodynamic sampler and the confluence of solutions in the microchannels were also evaluated by means of microscopy.

Experimental

Apparatus

A commercial photoexposer machine (Fotolight-MD2-A4, Carimbo Medeiros Ltda, Brazil), equipped with two sets of four mercury lamps (Black light F15W T12 Sylvania), was used to perform the exposure of the substrate to UV radiation. The photomasks were designed with the aid of AutoCad-2002 software (AutoDesk) and printed on an overhead transparency at a resolution of 1200 dpi with a laser printer (HP LaserJet 1300). An ultrasonic bath

(Branson model 2210) was employed to aid the rinsing of the exposed substrate in the development step.

To propel the solutions, miniature variable volume pumps, models LPVX 0502150 B (250 μL full stroke) and LPVX 0504950 B (750 μL full stroke), were purchased from the Lee Company (USA), presenting resolutions of 0.5 μL and 1.5 μL in the full-step operation mode, respectively. These pumps also work in the half-step mode, allowing inserting half of the volumes indicated above in each step. Mini-solenoid valves (model LHDA 0531415H), also acquired from the Lee Company, were used to control flow directions.

A controller module based on the microcontroller PIC 16F819 (microchip) was developed to automate all the operations of the microanalyzers and to trigger the photomultiplier (Hamamatsu H7468-03) during the analysis. Software written in Microsoft VisualBasic 5.0 (Microsoft) was employed to adjust the parameters of the photomultiplier and to store and plot the data generated by the analogical to digital converter (16 bits) integrated to the photomultiplier.

A USB-equipped digital microscope (Avantscope) was employed to acquire, in real time, images of the hydrodynamic sampling and of the confluence of solutions.

Reagents and solutions

The photoresin (Macdermid, Flexlight M050) was acquired from Carimpos Medeiros Ltda. Analytical-grade reagents and distilled/deionised water were used to prepare all solutions.

For the studies with fluorescein, a 0.4 mmol L^{-1} NaHCO_3 solution was prepared by dissolving the appropriate amount of the salt (Vetec) in water. A 1.33 mmol L^{-1} fluorescein stock solution was prepared by dissolving the reagent (Merck) in the NaHCO_3 solution. Fluorescein reference solutions in the range from 0.53 to 2.66 $\mu\text{mol L}^{-1}$ were prepared by proper dilution of the stock solution in 0.4 mmol L^{-1} NaHCO_3 .

For the determination of total Ca^{2+} and Mg^{2+} in mineral water, a 25 mmol L^{-1} Ca^{2+} stock solution was prepared by dissolving the appropriate quantity of dry CaCO_3 (Vetec) in 20.0 mL of 0.1 mol L^{-1} HCl, followed by dilution to 100 mL with water. Reference solutions containing 1.0 to 5.0 mg L^{-1} of Ca^{2+} (ca. 25 to 125 $\mu\text{mol L}^{-1}$) were prepared by proper dilution of the stock solution with 0.1 mol L^{-1} HCl. A 1,000 mg L^{-1} calcein (fluorexon) stock solution was prepared by dissolving the reagent (Acros) in 0.1 mol L^{-1} KOH solution, being stable for 1 week if kept in a refrigerator. The calcein solution (10 mg L^{-1}) used for the experiments was prepared daily by diluting the stock solution in 0.2 mol L^{-1} KOH solution. Commercial mineral waters were acquired in a local market and appropriately

diluted with deionised water, adjusting the concentration of HCl to 1 mmol L^{-1} .

Construction of the microsystems with integrated detection

The photolithographic process previously described for manufacturing a microanalyzer with an integrated photometric detection cell [17] was employed in the present work. This procedure consists basically of engraving the channels on a polymeric layer (2.0 mm of thickness) with subsequent sealing with another layer of the substrate, under controlled conditions. The regions to be engraved in the polymeric substrate were previously defined by masks made with laser printer transparency film.

Hypodermic needles (305111-BDTM) with external diameters of 0.45 mm were coupled to the channels previously engraved in the polymeric substrate in order to access the system. In a similar way, two plastic optical fibers (250 μm diameter, Toray, UK) were coupled to a 2.0-mm-long detection channel and used to guide the excitation radiation from an ultra-bright blue LED (acquired in the local market, maximum emission at 470 nm, bandwidth of 25 nm) to the microsystem. Another pair of optical fibers was adapted to the same detection channel, at a right angle, in order to collect the emitted radiation, conducting it to a photomultiplier, furnished with an optical filter (OA57 Scott glass color filter, maximum transmittance at 750 nm). Figure 1 shows photographs of the two devices constructed in the present work. Optical fibers were connected to the systems under pressure and in direct contact with the working solutions, avoiding leakage through the channels. To prevent effects of spurious radiation, the microsystem and the photomultiplier were placed in black plastic boxes.

Procedures

The studies with fluorescein were carried out in a single-line flow system, as shown in Fig. 2a. Reference and sample solutions were introduced into the device by means of hydrodynamic injection [18] using a sampling plug of 0.520 μL . A 0.40 mmol L^{-1} NaHCO_3 solution was used as carrier and the flow rate was fixed at 60 $\mu\text{L min}^{-1}$. The sampling step was performed with four mini-solenoid valves (V1–V4) turned on and both pumps (P1 and P2) working in the full-step mode for 20 s. During this procedure, the pumps were run in the aspiration mode, in order to refill P1 with the NaHCO_3 carrier solution, while the sampling loop was filled with the sample solution by actuation of pump P2. After sampling, all valves were turned off and both pumps started to operate in the reverse direction, in half-step mode, for 40 s. In this way, pump P1 impelled the sample with the carrier solution towards the detector for measurement, while P2 discharged solution to

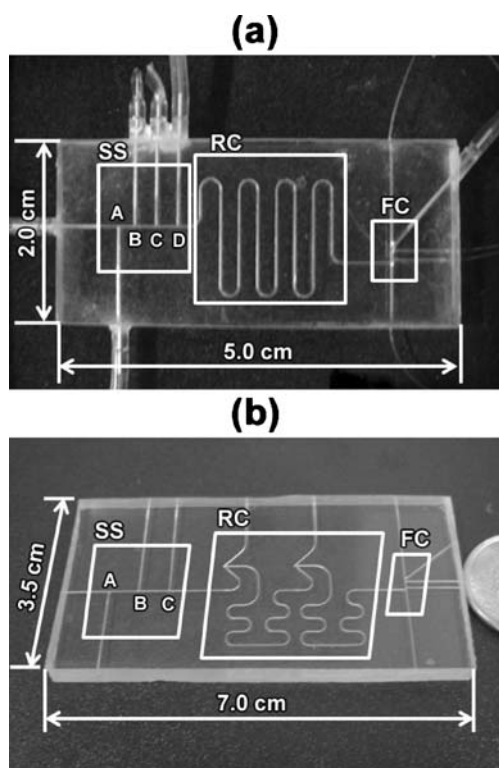


Fig. 1 Photographs of the proposed microsystems: **a** single-line FIA manifold and **b** microsystem with confluence points. *SS* sampling system, *RC* reaction coil, *FC* flow cell, *A* input of sample solution, *B*, *C*, and *D* output of sample solutions

waste, being prepared for the next sampling step. The software was adjusted to acquire the fluorescent signal (80 points per injection) while the sample plug was flowing through the detection cell.

To carry out the determination of total Ca^{2+} and Mg^{2+} in mineral water, a flow injection microsystem designed to perform the confluence of sample and reagent solutions was used, as shown in Fig. 2b. Hydrodynamic sampling was also employed to insert 2.40 μL of reference or sample solution into the device in a similar manner to that described in the study with fluorescein. Pumps P1 and P3 were used to propel the carrier (0.02 mol L^{-1} KOH) and the reagent (10 mg L^{-1} calcein) solutions, respectively, at the same flow rate of 60 $\mu\text{L min}^{-1}$, while P2 was used to aspirate the sample through valves V2 and V3. After sampling, P1 impelled the solution plug (SP) to the confluence point (P), where the sample solution was merged with the reagent stream. Afterwards, the solutions were mixed in the reaction coil (RC), while propelled to the fluorimetric flow cell (FC). The complete procedure was accomplished in 90 s (30 s for sampling and 60 s for reaction and data acquisition). Immediately after sampling, the data acquisition was started and performed in intervals of 0.3 s for 60 s, totaling to 200 data points for each sample injection.

Results and discussion

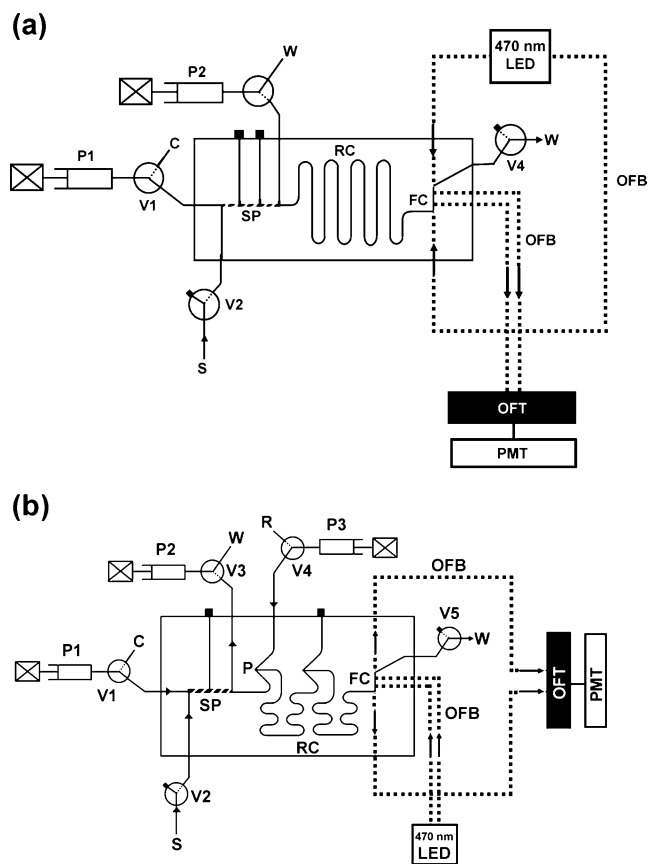
Characterization of the microsystems

Figure 1 shows the photographs of the devices, indicating that the sampling system (SS), reaction coil (RC), and fluorimetric cell (FC) are integrated in the monolithic UA systems, which are smaller than a credit card. The lengths and the volumes of these parts are listed in Table 1. In spite of the high number of optical fibers coupled to the detection channel, with distances smaller than 2.0 mm, no leakage was observed for flow rates up to 1.0 mL min^{-1} , demonstrating the efficiency of the seal.

As demonstrated earlier [17], the microchannels manufactured by the proposed technique present triangular cross sections with dimensions depending on the position of the photolithographic mask used and on the width of the printed lines of the mask. As a consequence, the single-line microsystem (Fig. 1a) presents channels with a width of 300 μm (triangle basis) and depth (triangle height) of 200 μm as well as channels with a width of 350 μm and depth of 370 μm . The microsystem with confluence point (Fig. 1b) presents channels 525 or 540 μm wide and 515 or 590 μm deep.

The volumes of the injection loops AB, AC, and AD, indicated in Table 1, were calculated based on the dimensions of the channels. The sample volume in the hydrodynamic injection approach is defined by the region between the input channel A and the output channel (B, C, or D in Fig. 1), which is chosen by the user before starting analysis. For the single-line device (Fig. 1a), real-time images were acquired for AB and AC loops during the sampling procedure of a 0.4 mol L^{-1} KMnO_4 solution, using a 5% (w/v) hydroxylamine chloride solution as carrier. Such high concentrations were necessary to provide adequate image contrast, making possible its visualization. Figure 3a shows the injection sequence for the smaller plug (0.13 μL , AB segment in Fig. 1a) obtained by using the same flow configuration depicted in Fig. 2a. As can be seen, the sample properly fills the 2.0-mm channel without exceeding the limits between the input and output channels (step 1), indicating a good performance of the proposed sampling procedure, which was performed by aspirating the permanganate solution at 300 $\mu\text{L min}^{-1}$. However, a significant enlargement of the sample zone was observed with loss of reproducibility when flow rates higher than 500 $\mu\text{L min}^{-1}$ were used to aspirate the solution. Such behavior is caused by the high pressure drop in the system that hinders the use of this sampling approach at high frequencies. As can be seen in Fig. 3b, sampling through the AC plug (0.32 μL) provided a similar performance, with sample solution not surpassing the pre-defined segment, even that previously obstructed by the user for volume selection (OC).

Fig. 2 **a** Single-line FIA manifold and **b** FIA manifold for determination of total Ca^{2+} and Mg^{2+} . *P1–P3*, piston pumps, *V1–V5* mini-solenoid valves (off mode), *SP* sample plug (hatched lines 0.52 μL for **(a)** and 2.40 μL for **(b)**); *RC* reaction coil, *FC* flow cell, *OFB* optical fibers, *OFT* optical filter (maximum transmittance at 750 nm), *PMT* photomultiplier, *S* sample, *C* carrier, *W* waste



The subsequent images (steps 2 and 3) depicted in Fig. 3 show the hydroxylamine solution carrying the sample plug of potassium permanganate solution. After sampling, the extremities of the loop instantly react with the carrier forming a colorless product, as a result of the dispersion of sample [19]. For the loop AC (Fig. 1a), it was observed that a small and reproducible aliquot of sample remains in the obstructed channel (OC), being completely removed by the carrier after ~ 2 s, not representing a problem for the proposed sampling approach, as indicated by the relative standard deviation of successive injections (2.0%) [17] (for more details, see electronic supplementary material, videos 1 and 2).

The flow injection microsystem applied to determination of Ca^{2+} and Mg^{2+} in mineral water (Fig. 1b) was fabricated to permit the confluence of solutions. In conventional flow injection analyzers, this approach is used to improve the mixture of fluids, allowing the injection of larger sample volumes, with consequent improvement of sensitivity [19]. Usually, confluence is implemented at a right angle that did not provide efficient mixing in the present work. Therefore, an alternative configuration was adopted to merge the solutions at the point P shown in Fig. 2b, in an attempt to increase flow turbulence and improve the mixing of the solutions. Microscopy images obtained at this point (Fig. 4), employing a 0.4 mol L^{-1} KMnO_4 solution and a

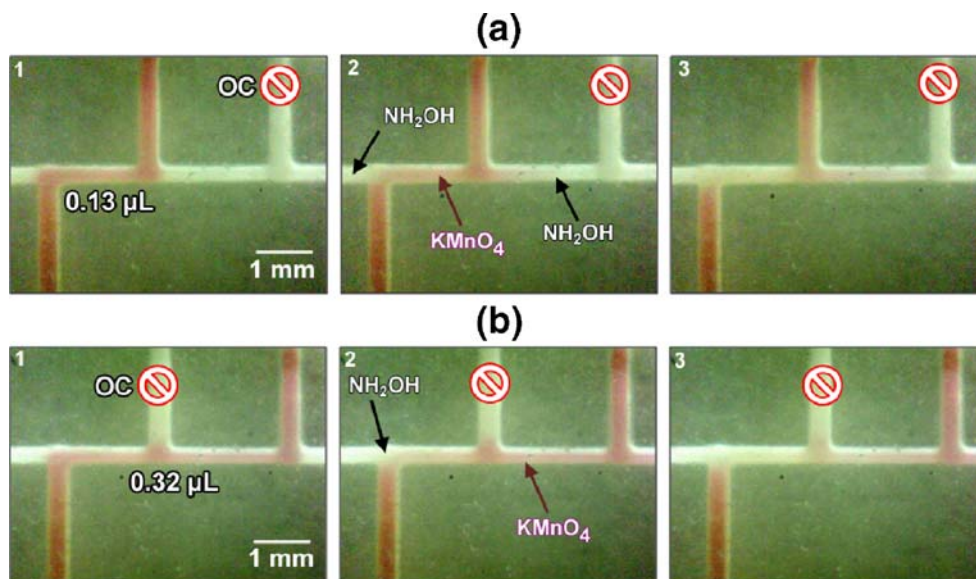
Table 1 Dimensions of the microfluidic systems

	Microsystem A ^a		Microsystem B ^a	
	Length (mm)	Volumes (μL)	Length (mm)	Volumes (μL)
AB loop	2.0	0.13	10.0	1.60
AC loop	5.0	0.32	15.0	2.40
AD loop	8.0	0.52		
Reaction coil	130	5.82	140	19.60
Flow Cell	2.0	0.08	2.0	0.26
Entire device ^b		10.4		37.90

^a Refers to the microsystems depicted in Fig. 1a and b

^b Access channels included

Fig. 3 Microscopy images of sampling procedure for the single-line FIA manifold depicted in Fig. 1a; **a** 0.13 μL sample loop; **b** 0.32 μL sample loop; *OC* obstructed channel. (1) Filled sample loop, (2–3) sample propelled by carrier



5% (w/v) hydroxylamine chloride solution apparently indicate that the mixing did not occur promptly, as both solutions were propelled side by side with no visible alteration until reaching the reaction coil, where the permanganate solution was decolorized. Such a performance confirmed the highly laminar flow regimen in micro-

channels, even under the proposed configuration for the confluence point. However, when the flow is stopped, permanganate solution is promptly decolorized, demonstrating the efficiency of mixing (see electronic supplementary material, video 3). In other words, the flow rate employed is high compared to diffusion rate of the analytes, providing a constant renewing of solutions in the region imaged, thus hiding the mixing process.

Fluorimetric determinations

The single-line flow analysis microsystem (Fig. 2a) was first evaluated regarding its integrated fluorimetric cell. Figure 5a shows the diagram obtained for injections of fluorescein reference solutions in the concentration range from 0.53 to 2.66 $\mu\text{mol L}^{-1}$ (peaks marked with a gray box must not be considered, as they are necessary for rinsing the sampling system when the sample is changed), while Fig. 5b represents the rescaled signal acquired for the injection of a 2.66 $\mu\text{mol L}^{-1}$ fluorescein solution. It can be noted that the transient signals are similar to those obtained by conventional FIA systems, indicating a similar dispersion of sample through the triangular microchannels. It can also be seen that the baseline exhibits a small drift, of ca. 50 arbitrary units after 15 min of analysis, which possibly arises as a consequence of the slight adsorption of the fluorophore on the channel walls. However, this does not impair the determination.

The adequate signal to noise ratios observed for injections of all reference solutions demonstrate that the proposed approach is feasible for fluorimetric detection in UA flow injection microsystems. The precision was evaluated by the peak heights for each set of sample injections with the same concentration, presenting a mean

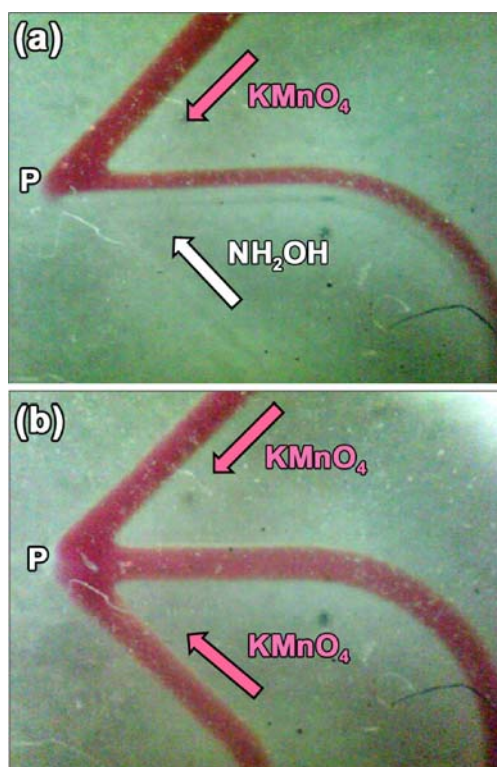


Fig. 4 Microscopy images acquired at the confluence point of the system depicted in Fig. 1b. **a** Merging of KMnO_4 solution with NH_2OH solution, **(b)** merging of two KMnO_4 solutions used for better visualization of the channels

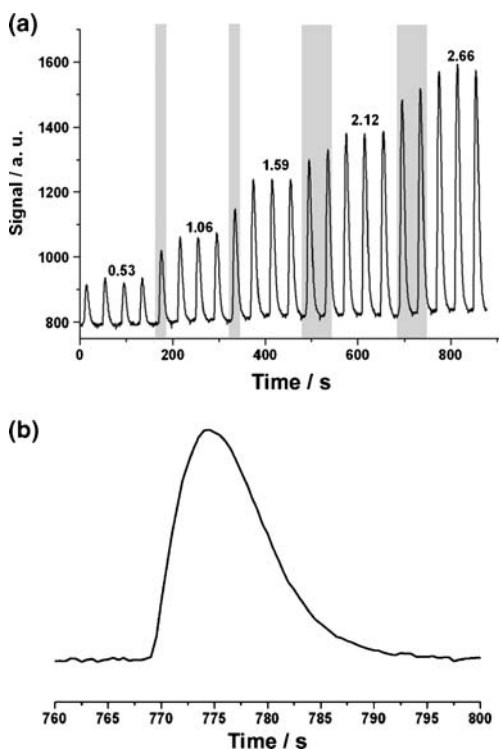


Fig. 5 Diagram for the injection of fluorescein reference solutions ($0.53\text{--}2.66\ \mu\text{mol L}^{-1}$; **a**) and rescaled signal for the injection of the $2.66\ \text{mg L}^{-1}$ reference solution (**b**). Peaks in gray refer to change of solutions

relative standard deviation of 1.9%. Assuming the total time required for injection and data acquisition described in experimental section, the analytical frequency is 60 samples h^{-1} . In addition, considering the flow rate for the carrier stream, $60\ \mu\text{L min}^{-1}$, a residue volume of only 3.2 mL is generated after an hour of work, representing an enormous improvement over conventional flow systems.

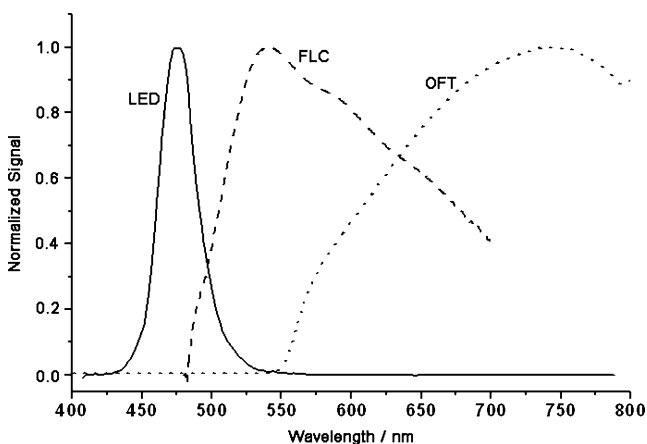


Fig. 6 Normalized spectra of the blue ultra-bright LED (maximum emission at 470 nm; LED), fluorescein emission excited at 470 nm (FLC), and the optical filter (OFT)

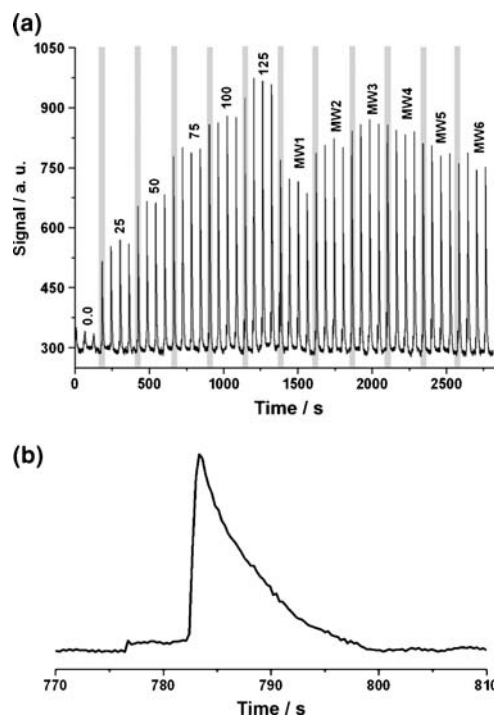


Fig. 7 Determination of total Ca^{2+} and Mg^{2+} in mineral waters. **a** Diagram and **b** rescaled signal for the injection of $75\ \mu\text{mol L}^{-1}$ reference solution. Peaks in gray refer to change of solutions

The analytical curve constructed from data shown in Fig. 5a showed a linear relationship ($r^2=0.996$), providing a limit of detection (LOD) of $0.37\ \mu\text{mol L}^{-1}$. Although this LOD is still high compared to that normally encountered for this determination ($0.80\ \text{nmol L}^{-1}$) [20], better results could be obtained by using a blue laser (470 nm) as excitation source and by changing the optical filter used to another with maximum transmittance at a lower wavelength. As indicated by the spectra of Fig. 6, the region of maximum transmittance of the optical filter does not match the wavelength of maximum emission of the fluorophore excited at 470 nm, so that the intensity of light that reaches

Table 2 Determination of total Ca^{2+} and Mg^{2+} in mineral waters

Sample	μFIA	Complexometric Titration	
	$[\text{Ca}^{2+}]+[\text{Mg}^{2+}]^{\text{a}}$ ($\mu\text{mol L}^{-1}$)	$[\text{Ca}^{2+}]+[\text{Mg}^{2+}]^{\text{b}}$ ($\mu\text{mol L}^{-1}$)	Deviation (%)
MW1	1170 ± 59	1020 ± 8	+14.0
MW2	837 ± 20	825 ± 5	+1.5
MW3	483 ± 7	460 ± 7	+5.1
MW4	453 ± 6	451 ± 1	+0.6
MW5	788 ± 24	822 ± 3	-4.1
MW6	143 ± 8	154 ± 2	-7.0

^a Average of three injections \pm standard deviation

^b Average of three determinations \pm standard deviation

the photomultiplier is strongly attenuated. It is necessary to emphasize that the use of the filter is indispensable, as some radiation of the blue LED is reflected by the channel walls and collected by optical fibers, generating high background signals if the filter is not used. In addition, the use of a filter with maximum transmittance at 525 nm also produces a high background signal as a consequence of the bandwidth of the blue LED [21]. Although the filter employed is not the most recommended, it is adequate to demonstrate the feasibility of the proposed detection system.

For the determination of total Ca^{2+} and Mg^{2+} in mineral waters, the position of the optical fibers (Fig. 2b) was inverted in relation to that used for detection of fluorescein (Fig. 2a). Preliminary experiments indicated a reduction of at least 50% of the baseline drift, with no alteration of signal profile. In fact, this configuration reduces the effects of the light emitted by the small amount of fluorophore adsorbed on the channel walls, as the collecting fibers are positioned parallel to the detection channel.

Figure 7a shows the fiagram acquired for the injection of reference and mineral water sample solutions using the proposed flow analysis microsystem (Figs. 1b and 2b). As can be seen, the baseline exhibits good stability with adequate signal to noise ratios. In spite of this, the transient signal for the injection of a $75 \mu\text{mol L}^{-1}$ Ca^{2+} reference solution (Fig. 7b) presents a different profile from the fluorescein peak (Fig. 5b). This different behavior arises from the fact that in the Ca^{2+} determination there is an on-line reaction, while the signal for fluorescein is not affected by a chemical reaction. This statement is supported by the fact that the injection of Ca^{2+} solution in the single-line FIA manifold (Fig. 2a) produces signals similar to that depicted in Fig. 7b, while the peak profiles for fluorescein are also identical, independent of the system employed for measurement.

The precision of the measurements was evaluated by the injection of five replicates of a $75 \mu\text{mol L}^{-1}$ Ca^{2+} reference solution, providing a relative standard deviation of 3.5%, a value that attests to the performance of the microsystem. Considering the time interval of 90 s necessary to inject the sample and acquire the respective data, the analytical frequency was estimated at $40 \text{ samples h}^{-1}$, which corresponds to 80% of the frequency provided by a conventional flow analyzer for similar determinations [22]. Despite this apparent disadvantage, the proposed microdevice produces $40 \mu\text{g}$ of calcein (ca. 7.2 mL of solution) after an hour of work, which represents a reduction of approximately 60 times in residue generation when compared to a conventional flow analyzer [22].

The analytical curve constructed from the data, shown in Fig. 7a, demonstrates a good linear relationship ($r^2=0.990$), providing a detection limit of $2.0 \mu\text{mol L}^{-1}$, which is a better

value than those reported for a conventional flow analyzer [22]. Table 2 lists the results obtained with the proposed microflow analyzer and those obtained by complexometric titration for the determination of the total Ca^{2+} and Mg^{2+} in mineral water. A plot of the results obtained by the proposed system against those obtained by titration provided a regression of “ $\mu\text{FIA} = (-44.6 \pm 162.7) + (1.11 \pm 0.22)$ titration” ($r^2=0.943$), that indicates there is no systematic error, as the linear coefficient and slope are close to zero and one, respectively.

Conclusions

The flow analysis microsystems proposed in this work were constructed rapidly and efficiently, using a simple procedure. The fluorimetric flow cells were successfully implemented, providing an easy way to perform the optical measurements in the microfluidic devices. The good performance presented for the determination of total Ca^{2+} and Mg^{2+} ions indicates that these microsystems can be a useful tool for other applications that also fit the aim of the green chemistry.

Acknowledgments Authors are grateful to CNPq (grant 479542/2004-0 and research fellowships) and to CAPES/PROCAD (grant 0081/05-1) for financial support and to Professor C.H. Collins for manuscript revision. A. Fonseca acknowledges UNICAMP for a fellowship.

References

- Dunec AF, Cheregi M, Calatayud JM, Mateo JVG, Eneim HYA (2003) *Crit Rev Anal Chem* 33(1):57–68
- Danet AF, Cheregi M, Calatayud JM, Mateo JVG, Eneim HYA (2001) *Crit Rev Anal Chem* 31(3):191–222
- Cerda V, Estela JM, Forteza R, Cladera A, Becerra E, Altimira P, Sitjar P (1999) *Talanta* 50(4):695–705
- Ruzicka H, Hansen EH (1984) *Anal Chim Acta* 161(1):1–25
- Becker H, Locascio LE (2002) *Talanta* 56(2):267–287
- Leelasattathkul T, Liawruagrath S, Rayanakorn M, Liawruagrath B, Oungpipat W, Youngvises N (2007) *Talanta* 72(1):126–131
- Madou MJ (1997) *Fundamentals of microfabrication*. CRC, Boca Raton
- Baeza MDM, Ibanez-Garcia N, Baucells J, Bartroli J, Alonso J (2006) *Analyst* 131(10):1109–1115
- Kruanetr S, Liawruagrath S, Youngvises N (2007) *Talanta* 73(1):46–53
- Kuswandi B, Nuriman HJ, Verboom W (2007) *Anal Chim Acta* 601(2):141–155
- Götz S, Karst U (2007) *Anal Bioanal Chem* 387(1):183–192
- Reyes DR, Iossifidis D, Auroux PA, Manz A (2002) *Anal Chem* 74(12):2623–2636
- Hata K, Kichise Y, Kaneta T, Imasaka T (2003) *Anal Chem* 75(7):1765–1768

14. Leach AM, Wheeler AR, Zare RN (2003) *Anal Chem* 75(4):967–972
15. Du W, Fang Q, Fang Z (2006) *Anal Chem* 78(18):6404–6410
16. Destandau E, Lefevre JP, Eddine ACF, Desportes S, Jullien MC, Hierle R, Leray I, Valeur B, Delaire JA (2007) *Anal Bioanal Chem* 387(8):2627–2632
17. Fonseca A, Raimundo IM Jr, Rohwedder JJR, Ferreira LOS (2007) *Anal Chim Acta* 603(2):159–166
18. Ruzicka J, Hansen EH (1983) *Anal Chim Acta* 145(1):1–15
19. Ruzicka J, Hansen EH (1981) *Flow injection analysis*. Wiley, New York
20. Hart SJ, Jiji RD (2002) *Anal Bioanal Chem* 374(3):385–389
21. Fonseca A, Raimundo IM Jr (2004) *Anal Chim Acta* 522(2):223–229
22. Chimpalee N, Chimpalee D, Jarungapattananon R, Lawratchavee SE, Burns DT (1993) *Anal Chim Acta* 271(2):247–251